Target and Equalizer Design for High-Density Bit-Patterned Media Recording

Santi Koonkarnkhai[1],
Phongsak Keeratiwintakorn[2], and **Piya Kovintavewat**[3], Non-members

ABSTRACT

In bit-patterned media recording (BPMR) channels, the inter-track interference (ITI) is extremely severe at ultra high areal densities, which significantly degrades the system performance. The partial-response maximum-likelihood (PRML) technique that uses an one-dimensional (1D) partial response target might not be able to cope with this severe ITI, especially in the presence of media noise and track mis-registration (TMR). This paper describes the target and equalizer design for high-density BPMR channels. Specifically, we proposes a two-dimensional (2D) cross-track asymmetric target, based on a minimum mean-squared error (MMSE) approach, to combat media noise and TMR. Results indicate that the proposed 2D target performs better than the previously proposed 2D targets, especially when media noise and TMR is severe.

Keywords: Bit-Patterned Media Recording (BPMR), Inter-Track Interference (ITI), Media Noise, Target and Equalizer Design, Track Mis-Registration (TMR)

1. INTRODUCTION

Currently, the perpendicular magnetic recording (PMR) technology is employed to store data in hard disk drives (HDDs). However, this technology will soon reach its maximum storage capacity at about 1 terabit per square inch (Tbit/in^2), known as the *super-paramagnetic limit* [1]. As a result, several technologies have been recently proposed to extend the storage capacity of next generation's HDDs [2], including heat-assisted magnetic recording (HAMR), microwave-assisted magnetic recording (MAMR), bit-patterned media recording (BPMR), and two-dimensional magnetic recording (TDMR).

The HAMR technology [3] is similar to the PMR technology, except that a laser is used to heat the medium during the writing process so as to reduce the medium coercivity. This leads to the lower magnetic field required in writing a data bit into a medium. Once the data bit has been written, the medium is rapidly cooled down until it reaches an ambient temperature. Although HAMR can achieve an areal density beyond 1 Tbit/in^2, there are still many challenges to be overcome before a real implementation can be deployed, including the development of an efficient light delivery system, thermo-magnetic write head, head-disk interface, cooling system, and so on [3]. Instead of using a laser, MAMR employs a microwave frequency [4]. Specifically, a high-frequency magnetic field is applied to a tiny spot of a medium so as to make the writing of magnetic information easy. Again, this MAMR technology is still under the development of a robust microwave oscillator [4].

In BPMR, each data bit is fabricated in exactly predefined locations in a medium, as opposed to a conventional medium where grain positions are random. In addition, a data bit is stored in a single domain magnetic island, which is surrounded by non-magnetic material. This helps reduce the transition noise, thus improving the signal-to-noise ratio (SNR) of the readback signal. Although the BPMR can increase an areal density up to 4 Tbit/in^2 [5], the process to create the islands at very high precision both location and shape is a challenge issue (i.e., BPMR requires a new medium structure).

Like HAMR and MAMR, TDMR can also employs the conventional media. Even though TDMR is a promising technology that can achieve an areal density up to 10 Tbit/in^2 [6] by storing one data bit using few grains in a magnetic medium, it needs a totally new design on both read and write processes. Additionally, a very advanced 2D signal processing technique must also be utilized for data detection.

Among all these technologies, this paper focuses on the BPMR technology because it offers a large areal density at moderate system change. At high areal densities, BPMR faces with new challenges in signal processing, such as 2D interference, media noise, track mis-registration (TMR), and so forth. The 2D interference consists of inter-symbol interference (ISI) and inter-track interference (ITI). Generally, the severity of ISI and ITI relies upon how far the islands are separated (i.e., a small bit period means high ISI, whereas a small track pitch represents high ITI). In

Manuscript received on August 11, 2011 ; revised on January 31, 2012.
[1,2] The authors are with Department of Electrical and Computer Engineering, King Mongkut's University of Technology North Bangkok, Thailand, E-mail: santi@npru.ac.th and phongsakk@kmutnb.ac.th
[3] The author is with Data Storage Technology Research Center, Nakhon Pathom Rajabhat University, Thailand, E-mail: pkovintavewat@yahoo.com
[3] Corresponding author (e-mail: piya@npru.ac.th)

practice, the conventional 1D equalizer and 1D target can handle the ISI [7, 8], but not the ITI. Therefore, at low areal density, the 1D target (low complexity) is sufficient to be used in data detection process because it can provide similar performance if compared to the 2D target (high complexity). On the other hand, when the areal density is high, the system will experience severe ISI and ITI. In this case, it is unavoidable to employ the 2D target so as to alleviate both ISI and ITI effectively [1].

In addition to the ISI and ITI, there is also an impact from media noise and TMR in the BPMR system. Media noise is resulted from non-uniform magnetic islands with amplitude fluctuation and location fluctuation, whereas the TMR is a read-head offset occurred when the read head is not aligned at the center of the main track. Furthermore, the write synchronization error in BPMR also leads to the problem of insertion/deletion and substitution in the readback signal, which significantly degrades the system performance, but this issue is out of scope here.

Many works have been proposed for data detection in BPMR systems. Nabavi *et al.* [9] proposed the modified Viterbi detector, which uses the same trellis diagram as employed in a conventional (1D) Viterbi detector, to mitigate the ITI effect, and also to alleviate the TMR effect [9]. Then, Nabavi *et al.* [10] has also proposed the 1D target and 2D equalizer design for a multi-head BPMR system. It has shown that the 2D equalizer yields better performance than 1D equalizer at the expense of increasing complexity. Kalakulak [11] proposed a new channel model for designing the 1D equalizer and the 2D target with zero corner entries. Finally, Myint *et al.* [12] proposed an iterative decoding scheme to mitigate the ITI effect for a multi-head BPMR channel.

For the BPMR system with one read head, all recently proposed targets yield good performance at low areal densities (≤ 2.5 Tbit/in^2), but perform unreliable at high areal densities because of severe ITI. To combat this severe ITI, Koonkarnkhai *et al.* [13] proposed the design of symmetric 2D target and an iterative decoding scheme to combat severe ITI. However, the symmetric 2D target is not suitable for the system that experiences media noise and TMR. Therefore, this paper presents the target and equalizer design for high-density BPMR channels. Specifically, we propose the design of 2D cross-track asymmetric target based on a minimum mean-squared error (MMSE) approach, where the coefficients of the proposed 2D target are all different. We also compare the performance of the proposed 2D target with the existing 2D targets in terms of bit-error rate (BER) in the BPMR system with media noise and TMR.

This paper is organized as follows. After describing a BPMR channel model in Section 2, Section 3 presents the design of the target and its corresponding equalizer for BPMR channels. Simulation results

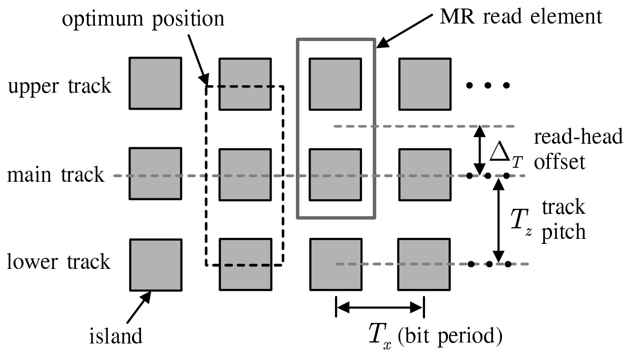

Fig.1: *A BPM channel model based on a square grid of islands with MR read-head.*

are given in Section 4. Finally, Section 5 concludes this paper.

2. CHANNEL MODEL

Consider the BPMR channel, where the 2D numerical pulse response is obtained based on the parameters of the media and the magneto-resistive (MR) head given in Table 1 [1]. Then, the 2D pulse response can be approximated by a 2D Gaussian pulse with media noise according to [1]

$$H(z,x) = (A+\Delta_A)\exp\left(-\frac{1}{2}\left[\left(\frac{x+\Delta_x}{c(W_x+\Delta_{W_x})}\right)^2 + \left(\frac{z+\Delta_z}{c(W_z+\Delta_{W_z})}\right)^2\right]\right), \quad (1)$$

where $A = 1$ is the maximum amplitude, Δ_A is the amplitude fluctuation, Δ_x is the along-track location fluctuation, Δ_z is the cross-track location fluctuation, W_x is the PW$_{50}$ of an along-track pulse, W_z is the PW$_{50}$ of a cross-track pulse, Δ_{W_x} is the along-track PW$_{50}$ fluctuation, W_z is the cross-track PW$_{50}$ fluctuation, and $c = 1/2.3458$ is a constant to account for the relationship between PW50 and the standard deviation of a Gaussian function. We rearrange the islands in a square grid as displayed in Fig. 1 by parameters T_x and T_z to achieve different areal densities according to [14]

$$\texttt{Areal density} \approx \frac{10^6}{1550 T_x T_z}, \quad (2)$$

in Tbit/in^2, where T_x is a bit period in nm on along-track direction and T_z is a track pitch in nm on cross-track direction.

Fig. 2 shows a channel model in the presence of media noise and TMR. An input sequence $a_{m,k} \in \pm 1$, where $m = 0$ is the main track, and $m = -1$ and $+1$ are an upper track and a lower track, respectively.

Table 1: *Media and MR head parameters used in a BPMR channel [1].*

Parameter	Symbol	Default value (nm)
Square island (each side)	a	11
Thickness	δ	10
Fly height	d	10
Thickness of the MR head	t	4
Width of the MR head	W	16
Gap to gap width	g	16
Along-track PW_{50}	W_x	19.8
Cross-track PW_{50}	W_z	24.8

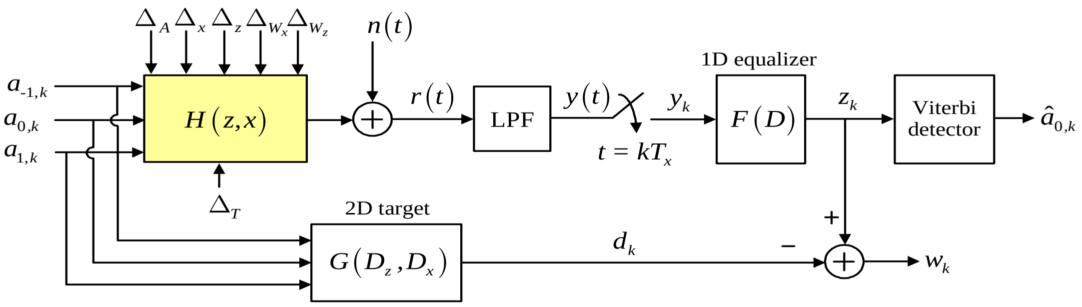

Fig.2: *A channel model with 1D equalizer and 2D target design in the presence of media noise and TMR.*

The readback signal $r(t)$ can then be written as [1]

$$r(t) = \sum_{m=-1}^{1} \sum_{k=-\infty}^{\infty} a_{m,k} H(-mT_z - \Delta_T, t - kT_x) + n(t), \tag{3}$$

where $n(t)$ is additive white Gaussian noise (AWGN) with two-sided power spectral density $N_0/2$. The TMR is defined as

$$\text{TMR} = \frac{\Delta_T}{T_z} \times 100\%, \tag{4}$$

where Δ_T is a track offset. The media noise (i.e., Δ_A, Δ_x, Δ_z, Δ_{W_x} and Δ_{W_z}) is modeled as a truncated Gaussian probability distribution function with zero mean and σ^2, where σ is specified as percentage of T_x.

The readback signal $r(t)$ is fed to a 7th-order Butterworth low-pass filter (LPF) and is sampled at $t = kT_x$, assuming perfect synchronization. Then, a sequence y_k is equalized by a 1D equalizer $F(D)$ to obtain a sequence z_k, and is fed to the Viterbi detector to determine the most likely input sequence $a_{0,k}$.

3. TARGET AND EQUALIZER DESIGN

In BPMR, the target and equalizer design is of importance to improve the system performance because it can help reduce the effect of both ISI and ITI. At low areal densities, the ITI effect is very small and can be neglected. On the other hand, when the areal density is high, the ITI effect is very severe and thus cannot be discarded when designing the target and its corresponding equalizer.

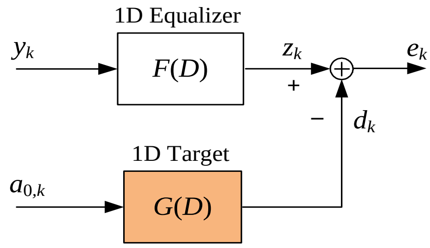

Fig.3: *The conventional 1D target and 1D equalizer design for BPMR channel.*

Here, we explain the design of the conventional 1D target, zero-corner 2D target, cross-track symmetric 2D target [13], and cross-track asymmetric 2D target.

3.1 Conventional 1D target design

Fig. 3 illustrates the model for the conventional 1D target and 1D equalizer design for BPMR channel. The 1D target $G(D)$ and its corresponding equalizer $F(D)$ are simultaneously designed based on the minimum mean-squared error (MMSE) approach. This can be achieved by minimizing

$$E[e_k^2] = E[(\mathbf{f}^T\mathbf{y}_k - \mathbf{g}^T\mathbf{a}_k)(\mathbf{f}^T\mathbf{y}_k - \mathbf{g}^T\mathbf{a}_k)^T], \tag{5}$$

where $e_k = z_k - d_k$, $*$ is a convolution operator, and $E[.]$ is an expectation operator. Let $\mathbf{g} = [g_{0,0} \quad g_{0,1} \quad g_{0,2}]^T$ is a column vector of the 1D target $G(D)$, where $g_{0,1}$ is set to 1, $\mathbf{f} = [f_{-K} \ldots f_0 \ldots f_K]^T$ is a column vector of the 1D equalizer $F(D)$, $\mathbf{y}_k = [y_{k+K} \ldots y_k \ldots y_{k-K}]^T$ is a column vector of the readback signal $\{y_k\}$, and

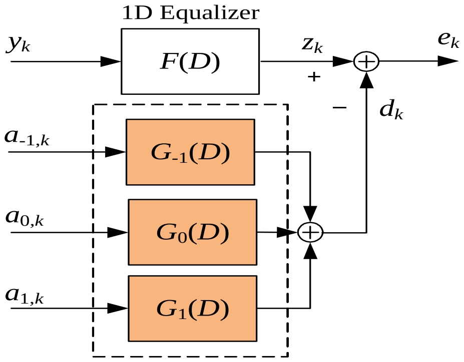

Fig.4: *The 2D target and 1D equalizer design for BPMR channel.*

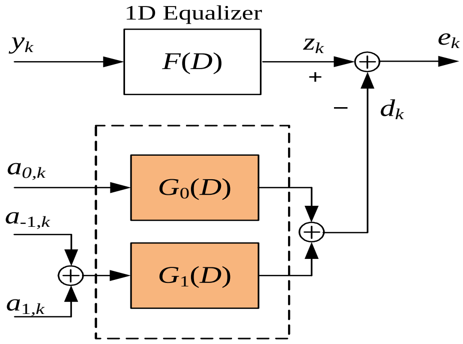

Fig.5: *The cross-track symmetric 2D target and 1D equalizer design for BPMR channel.*

$\mathbf{a}_k = [a_{0,k} \quad a_{0,k-1} \quad a_{0,k-2}]^{\mathrm{T}}$ is a column vector of the data input in the main track $\{a_{0,k}\}$, where $N = 2K+1$ is the number of equalizer coefficients, and $[.]^{\mathrm{T}}$ is the transpose operation. During the minimization process, we use a monic constraint of $\mathbf{I}^{\mathrm{T}}\mathbf{g} = 1$ to avoid reaching the trivial solutions of $\mathbf{g} = \mathbf{f} = \mathbf{0}$. Thus, (5) can be written as

$$E[e_k^2] = \mathbf{f}^{\mathrm{T}}\mathbf{R}\mathbf{f} + \mathbf{g}^{\mathrm{T}}\mathbf{A}\mathbf{g} - 2\mathbf{f}^{\mathrm{T}}\mathbf{T}\mathbf{g} - 2\lambda(\mathbf{I}^{\mathrm{T}}\mathbf{g} - 1), \quad (6)$$

where λ is a Lagrange multiplier, $\mathbf{I} = [0 \quad 1 \quad 0]^{\mathrm{T}}$, $\mathbf{R} = E[\mathbf{y}_k\mathbf{y}_k^{\mathrm{T}}]$ is an N-by-N autocorrelation of a sequence $\{y_k\}$, $\mathbf{T} = E[\mathbf{y}_k\mathbf{a}_k^{\mathrm{T}}]$ is an N-by-L of cross-correlation of sequences $\{y_k\}$ and $\{a_{0,k}\}$, $\mathbf{A} = E[\mathbf{a}_k\mathbf{a}_k^{\mathrm{T}}]$ is an L-by-L autocorrelation of a sequence $\{a_{0,k}\}$, and $L = 3$ is the target length. By differentiating (6) with respect to λ, $\mathbf{g}$ and $\mathbf{f}$, and setting the results to be zero, one obtains

$$\lambda = \frac{1}{\mathbf{I}^{\mathrm{T}}(\mathbf{A} - \mathbf{T}^{\mathrm{T}}\mathbf{R}^{-1}\mathbf{T})^{-1}\mathbf{I}}, \quad (7)$$

$$\mathbf{g} = \lambda(\mathbf{A} - \mathbf{T}^{\mathrm{T}}\mathbf{R}^{-1}\mathbf{T})^{-1}\mathbf{I}, \quad (8)$$

$$\mathbf{f} = \mathbf{R}^{-1}\mathbf{T}\mathbf{g}. \quad (9)$$

3.2 Zero-corner 2D target design

The model for the zero-corner 2D target and the 1D equalizer design is shown in Fig. 4. The equalizer output is a sequence $z_k = y_k * f_k = \mathbf{f}^{\mathrm{T}}\mathbf{y}_k$, where $\mathbf{f} = [f_{-K} \ldots f_0 \ldots f_K]^{\mathrm{T}}$ denote the 1D equalizer $F(D)$, and $\mathbf{y}_k = [y_{k+K} \ldots y_k \ldots y_{k-K}]^{\mathrm{T}}$ is a column vector of the readback signal $\{y_k\}$, where $N = 2K+1$ is the number of equalizer coefficients. The output of the 2D target with zero-corner entries is expressed as $d_k = a_{m,k} \circledast g_{m,k} = \mathbf{g}^{\mathrm{T}}\mathbf{a}_k$, where $\circledast$ is a 2D convolution operator [14], $\mathbf{a}_k = [a_{0,k} \quad a_{-1,k-1} \quad a_{0,k-1} \quad a_{1,k-1} \quad a_{0,k-2}]^{\mathrm{T}}$ is is a column vector of the data input $\{a_{m,k}\}$.

As illustrated in Fig. 4, we assume that the 2D target with zero-corner entries can be written in a matrix form of

$$\mathbf{G} = \begin{bmatrix} 0 & g_{-1,1} & 0 \\ g_{0,0} & g_{0,1} & g_{0,2} \\ 0 & g_{1,1} & 0 \end{bmatrix}. \quad (10)$$

Let $\mathbf{g} = [g_{0,0} \quad g_{-1,1} \quad g_{0,1} \quad g_{1,1} \quad g_{0,2}]^{\mathrm{T}}$ be a column vector of the 2D target with zero-corner entries, where $g_{0,1}$ is set to 1. Again, the 2D target $G(D)$ and its corresponding 1D equalizer $F(D)$ can be obtained by minimizing the mean-squared error between sequences z_k and d_k, which can be expressed as

$$E[e_k^2] = E[(\mathbf{f}^{\mathrm{T}}\mathbf{y}_k - \mathbf{g}^{\mathrm{T}}\mathbf{a}_k)(\mathbf{f}^{\mathrm{T}}\mathbf{y}_k - \mathbf{g}^{\mathrm{T}}\mathbf{a}_k)^{\mathrm{T}}], \quad (11)$$

To minimize (11), we impose a monic constraint of $\mathbf{I}^{\mathrm{T}}\mathbf{g} = 1$ to avoid reaching trivial solutions of $\mathbf{f} = \mathbf{g} = \mathbf{0}$. Therefore, $\mathbf{f}$ and $\mathbf{g}$ are chosen such that

$$E[e_k^2] = \mathbf{f}^{\mathrm{T}}\mathbf{R}\mathbf{f} + \mathbf{g}^{\mathrm{T}}\mathbf{A}\mathbf{g} - 2\mathbf{f}^{\mathrm{T}}\mathbf{T}\mathbf{g} - 2\lambda(\mathbf{I}^{\mathrm{T}}\mathbf{g} - 1), \quad (12)$$

is minimized, where $\mathbf{I} = [0 \ 0 \ 1 \ 0 \ 0]^{\mathrm{T}}$, $\mathbf{R} = E[\mathbf{y}_k\mathbf{y}_k^{\mathrm{T}}]$ is an N-by-N autocorrelation of a sequence $\{y_k\}$, $\mathbf{T} = E[\mathbf{y}_k\mathbf{a}_k^{\mathrm{T}}]$ is an N-by-L of cross-correlation of sequences $\{y_k\}$ and $\{a_{m,k}\}$, $\mathbf{A} = E[\mathbf{a}_k\mathbf{a}_k^{\mathrm{T}}]$ is an L-by-L autocorrelation of a sequence $\{a_{m,k}\}$, and $L = 5$ is the target length. The minimization process yields

$$\lambda = \frac{1}{\mathbf{I}^{\mathrm{T}}(\mathbf{A} - \mathbf{T}^{\mathrm{T}}\mathbf{R}^{-1}\mathbf{T})^{-1}\mathbf{I}}, \quad (13)$$

$$\mathbf{g} = \lambda(\mathbf{A} - \mathbf{T}^{\mathrm{T}}\mathbf{R}^{-1}\mathbf{T})^{-1}\mathbf{I}, \quad (14)$$

$$\mathbf{f} = \mathbf{R}^{-1}\mathbf{T}\mathbf{g}. \quad (15)$$

3.3 Cross-track symmetric 2D target design

Fig. 5 displays the model for the 2D target with cross-track symmetry and the 1D equalizer design. The 2D target is given in a 3-by-3 matrix form as

$$\mathbf{G} = \begin{bmatrix} G_{-1}(D) \\ G_0(D) \\ G_1(D) \end{bmatrix} = \begin{bmatrix} g_{-1,0} & g_{-1,1} & g_{-1,2} \\ g_{0,0} & g_{0,1} & g_{0,2} \\ g_{1,0} & g_{1,1} & g_{1,2} \end{bmatrix}, \quad (16)$$

where $G_{-1}(D) = G_1(D)$. The difference between z_k and d_k can be written as $e_k = z_k - d_k = f_k * y_k - g_{m,k} \circledast a_{m,k}$. Let $\mathbf{g} = [g_{-1,0} \quad g_{0,0} \quad g_{-1,1} \quad g_{0,1} \quad g_{-1,2} \quad g_{0,2}]^{\mathrm{T}}$ be an L-element column vector of $\mathbf{G}$, where $g_{0,1}$ is set to 1, $\mathbf{f} = [f_{-K} \ \ldots \ f_0 \ \ldots \ f_K]^{\mathrm{T}}$ be an N-element column vector of $F(D)$, $\mathbf{a}_k = [(a_{-1,k} + a_{1,k})$

$a_{0,k}$ $(a_{-1,k-1}+a_{1,k-1})$ $a_{0,k-1}$ $(a_{-1,k-2}+a_{1,k-2})$ $a_{0,k-2})]^{\mathrm{T}}$ be an L-element column vector of an input data sequence $\{a_{m,k}\}$, and $\mathbf{y}_k = [y_{k+K} \ldots y_k \ldots y_{k-K}]^{\mathrm{T}}$ be an N-element column vector of a sampler output sequence $\{y_k\}$, where $N = 2K+1$ is the number of equalizer coefficients. Thus, the mean-squared error of e_k can be expressed as

$$E[e_k^2] = E[(\mathbf{f}^{\mathrm{T}}\mathbf{y}_k - \mathbf{g}^{\mathrm{T}}\mathbf{a}_k)(\mathbf{f}^{\mathrm{T}}\mathbf{y}_k - \mathbf{g}^{\mathrm{T}}\mathbf{a}_k)^{\mathrm{T}}]. \quad (17)$$

During the minimization process, we use a constraint of $\mathbf{I}^{\mathrm{T}}\mathbf{g} = 1$ to avoid reaching solutions of $\mathbf{f} = \mathbf{g} = \mathbf{0}$, where $\mathbf{I} = [0\ 0\ 0\ 1\ 0\ 0]^{\mathrm{T}}$. Consequently, adding this constraint to (17) yields

$$E[e_k^2] = \mathbf{f}^{\mathrm{T}}\mathbf{R}\mathbf{f} + \mathbf{g}^{\mathrm{T}}\mathbf{A}\mathbf{g} - 2\mathbf{f}^{\mathrm{T}}\mathbf{T}\mathbf{g} - 2\lambda(\mathbf{I}^{\mathrm{T}}\mathbf{g} - 1), \quad (18)$$

where $\mathbf{A} = E[\mathbf{a}_k\mathbf{a}_k^{\mathrm{T}}]$, is an L-by-L autocorrelation matrix of a sequence $\{a_{m,k}\}$, $\mathbf{R} = E[\mathbf{y}_k\mathbf{y}_k^{\mathrm{T}}]$ is an N-by-N autocorrelation matrix of a sequence $\{y_k\}$, and $\mathbf{T} = E[\mathbf{y}_k\mathbf{a}_k^{\mathrm{T}}]$ is an N-by-L cross-correlation matrix of sequences $\{y_k\}$ and $\{a_{m,k}\}$, and $L = 6$ is the target length. Consequently, the minimization process yields

$$\lambda = \frac{1}{\mathbf{I}^{\mathrm{T}}(\mathbf{A} - \mathbf{T}^{\mathrm{T}}\mathbf{R}^{-1}\mathbf{T})^{-1}\mathbf{I}}, \quad (19)$$

$$\mathbf{g} = \lambda(\mathbf{A} - \mathbf{T}^{\mathrm{T}}\mathbf{R}^{-1}\mathbf{T})^{-1}\mathbf{I}, \quad (20)$$

$$\mathbf{f} = \mathbf{R}^{-1}\mathbf{T}\mathbf{g}. \quad (21)$$

3.4 Cross-track asymmetric 2D target design

The model for the 2D target with cross-track *asymmetry* and the 1D equalizer design is also illustrated in Fig. 4, where the 2D target is given in (16) with $G_{-1}(D) \neq G_1(D)$. As shown in Fig. 4, the difference between d_k and z_k is given by $e_k = z_k - d_k = y_k * f_k - a_{m,k} \circledast g_{m,k}$, where f_k is the k-th coefficient of an equalizer, and $N = 2K+1$ is the number of equalizer taps. The column vectors of the 2D target and the equalizer can be defined as $\mathbf{g} = [g_{-1,0}\ \ g_{0,0}\ \ g_{1,0}\ \ g_{-1,1}\ \ g_{0,1}\ \ g_{1,1}\ \ g_{-1,2}\ \ g_{0,2}\ \ g_{1,2}]^{\mathrm{T}}$, and $\mathbf{f} = [f_{-K} \ldots f_0 \ldots f_K]^{\mathrm{T}}$, respectively. Then, a mean square error of e_k can be expressed as

$$E[e_k^2] = E[(\mathbf{f}^{\mathrm{T}}\mathbf{y}_k - \mathbf{g}^{\mathrm{T}}\mathbf{a}_k)(\mathbf{f}^{\mathrm{T}}\mathbf{y}_k - \mathbf{g}^{\mathrm{T}}\mathbf{a}_k)^{\mathrm{T}}], \quad (22)$$

where $\mathbf{a}_k = [a_{-1,k}\ \ a_{0,k}\ \ a_{1,k}\ \ a_{-1,k-1}\ \ a_{0,k-1}\ \ a_{1,k-1}\ \ a_{-1,k-2}\ \ a_{0,k-2}\ \ a_{1,k-2}]^{\mathrm{T}}$ is a column vector of the input sequence $\{a_{m,k}\}$, and $\mathbf{y}_k = [y_{k+K} \ldots y_k \ldots y_{k-K}]^{\mathrm{T}}$ is a column vector of a sampler sequence $\{y_k\}$. To minimize (22), we impose a monic constraint of $\mathbf{I}^{\mathrm{T}}\mathbf{g} = 1$ to avoid reaching trivial solutions of $\mathbf{f} = \mathbf{g} = \mathbf{0}$. Therefore, $\mathbf{f}$ and $\mathbf{g}$ are chosen such that

$$E[e_k^2] = \mathbf{f}^{\mathrm{T}}\mathbf{R}\mathbf{f} + \mathbf{g}^{\mathrm{T}}\mathbf{A}\mathbf{g} - 2\mathbf{f}^{\mathrm{T}}\mathbf{T}\mathbf{g} - 2\lambda(\mathbf{I}^{\mathrm{T}}\mathbf{g} - 1), \quad (23)$$

is minimized, where $\mathbf{I} = [0\ 0\ 0\ 0\ 1\ 0\ 0\ 0\ 0]^{\mathrm{T}}$, $\mathbf{A} = E[\mathbf{a}_k\mathbf{a}_k^{\mathrm{T}}]$ is an L-by-L autocorrelation matrix of a sequence $\{a_{m,k}\}$, $\mathbf{R} = E[\mathbf{y}_k\mathbf{y}_k^{\mathrm{T}}]$ is an N-by-N autocorrelation matrix of a sequence $\{y_k\}$, and $\mathbf{T} = E[\mathbf{y}_k\mathbf{a}_k^{\mathrm{T}}]$ is an N-by-L cross-correlation matrix of sequences $\{y_k\}$ and $\{a_{m,k}\}$, where $L = 9$ is the target length. The minimization process yields

$$\lambda = \frac{1}{\mathbf{I}^{\mathrm{T}}(\mathbf{A} - \mathbf{T}^{\mathrm{T}}\mathbf{R}^{-1}\mathbf{T})^{-1}\mathbf{I}}, \quad (24)$$

$$\mathbf{g} = \lambda(\mathbf{A} - \mathbf{T}^{\mathrm{T}}\mathbf{R}^{-1}\mathbf{T})^{-1}\mathbf{I}, \quad (25)$$

$$\mathbf{f} = \mathbf{R}^{-1}\mathbf{T}\mathbf{g}. \quad (26)$$

4. NUMERICAL RESULT

Consider the BPMR channel in Fig. 2. We define a signal-to-noise ratio (SNR) as $20\log_{10}(1/\sigma)$ in decibel (dB). The 2D 3×3 target and 15-tap 1D equalizer are designed based on a MMSE approach [8]. In simulation, each BER is computed based on a minimum number of 500 error bits, and the 2D target and its corresponding 1D equalizer are designed in the presence of media noise and TMR at the SNR required to achieve BER = 10^{-4}.

Furthermore, several targets will be compared in this study. Specifically, we define the system using a 1D target and a conventional (1D) Viterbi detector as "1DTarget"; the system using a zero-corner 2D target and a modified Viterbi detector proposed in [10] as "Zero-corner 2D target"; the system using a cross-track symmetric 2D target (i.e., $\mathbf{G}_{-1}(D) = \mathbf{G}_1(D)$) and the 2D Viterbi detector (with 36 states and 6 branches) [11] as "Symmetric 2D target"; and the system using the proposed 2D target and the 2D Viterbi detector (with 64 states and 8 branches) [11] as "Asymmetric 2D target." Fig. 6 compares the performance of different targets at areal densities of 2 and 3 Tbit/in^2 with 0% media noise and 0% TMR, where $T_x = T_z = 18$ nm at 2 Tbit/in^2 and $T_x = T_z = 14.5$ nm at 3 Tbit/in^2, respectively. We found that at 2 Tbit/in^2, "Zero-corner 2D target" performs best, followed by "1D target," and the other 2D targets. The reason that "Symmetric 2D target" and "Asymmetric 2D target" perform worse than "1D target" and "Zero-corner 2D target" might be because the target with a large number of coefficients is more sensitive to disturbances than that with a less number of coefficients. Also, the ITI is not as severe as ISI and AWGN at 2 Tbit/in^2. However, at 3 Tbit/in^2 when ITI is very severe, it is clear that "Symmetric 2D target" and "Asymmetric 2D target" perform better than the others. Therefore, "Symmetric 2D target" and "Asymmetric 2D target" should be employed in the system with severe ITI.

Next, we consider the areal density of 3 Tbit/in^2. Then, we illustrate the performance of different targets at various media noise amounts and 0% TMR in Fig. 7, by plotting the SNR required to achieve BER = 10^{-4} as a function of media noise amounts. Apparently, media noise degrades the system performance. In addition, we see that "Asymmetric 2D target" performs best, followed by "Symmetric 2D target" and

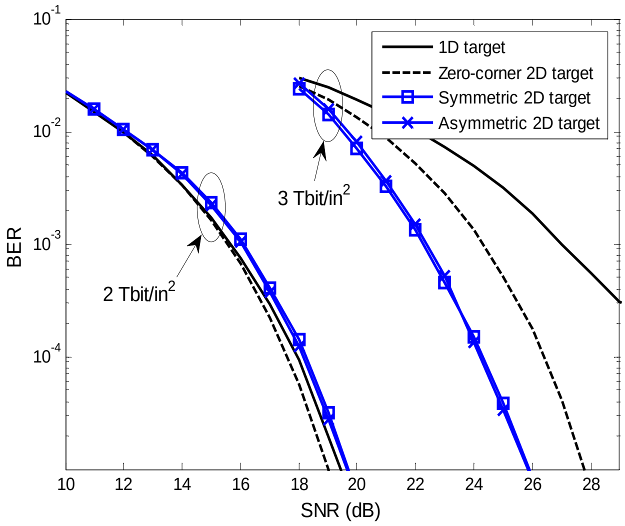

Fig. 6: *BER performance of different targets with 0% media noise and 0% TMR.*

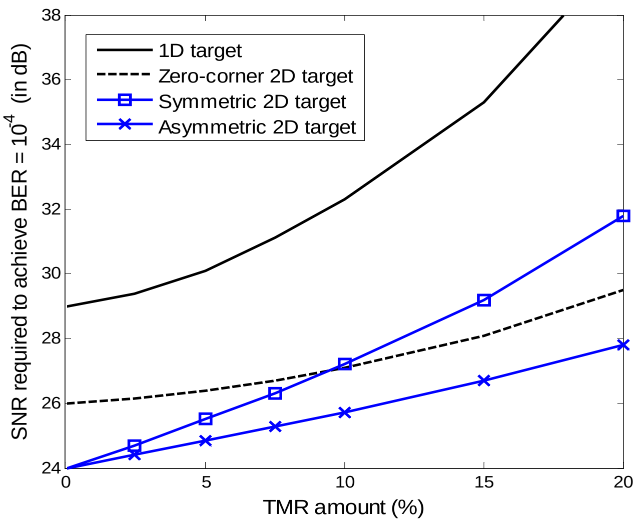

Fig. 8: *Performance comparison of different TMR amounts with 0% media noise.*

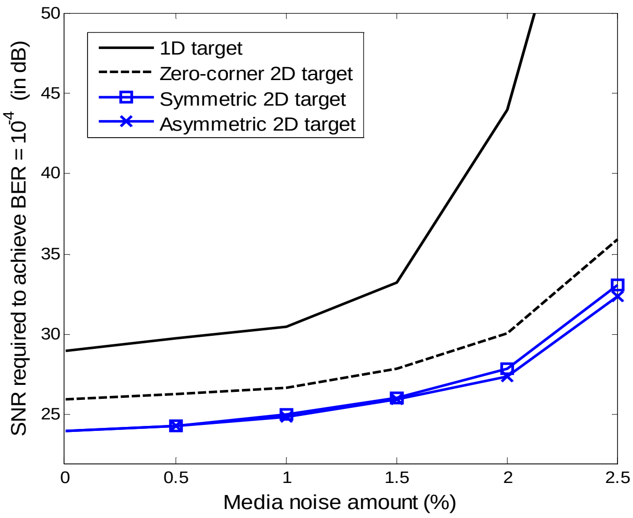

Fig. 7: *Performance comparison of different media noise amounts with 0% TMR.*

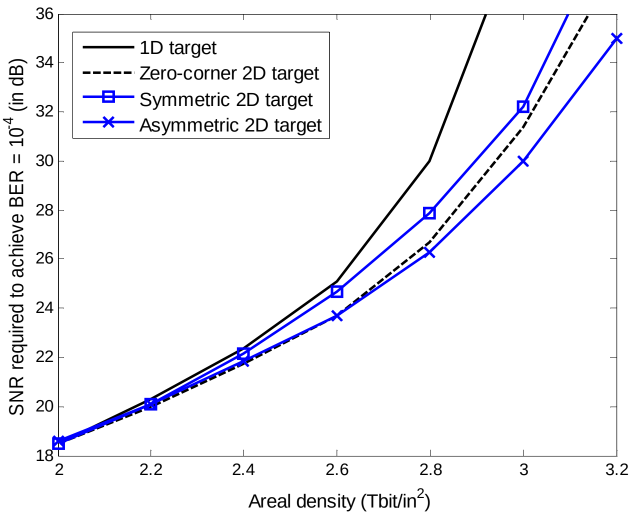

Fig. 9: *Performance comparison at different areal densities with 2% media noise and 10% TMR.*

the other two targets, especially when media noise is high. Again, the reason that "Asymmetric 2D target" yields slightly better performance than "Symmetric 2D target" is because the 2D pulse response in (1) is no longer symmetric in the presence of media noise.

We also compare the performance of different targets with various TMR amounts and 0% media noise in Fig. 8. Similarly, when TMR occurs, it causes the 2D pulse response in (1) to be asymmetric. Hence, it is expected that "Asymmetric 2D target" should perform better than "Symmetric 2D target" as depicted in Fig. 8. Furthermore, when TMR is severe (e.g., greater than 10%), we can see that "Zero-corner 2D target" is also better than "Symmetric 2D target," which might be because the target with a fewer number of coefficients is less sensitive to severe TMR than that with a larger number of coefficients.

Finally, Fig. 9 illustrates the performance comparison of different targets comparison at different areal densities with 2% media noise and 10% TMR. In this case, we found that "Asymmetric 2D target" performs the best if compared to other targets, especially at high areal densities.

Although it is apparent that "Asymmetric 2D target" performs better than other targets, it has very high complexity. Assuming that the system complexity depends solely on the complexity of the Viterbi detectors used in each scheme. Therefore, Table 2 compares the complexity of different detectors in terms of the number of trellis states and branch metrics [7]. In general, the larger the number of trellis states and branch metrics, the higher the complexity of the detector. Clearly, "1D target" has the lowest complexity if compared to other targets. On the other hand, "Asymmetric 2D target" (or, equivalently, the 2D full-complexity Viterbi detector) has the highest

Table 2: *Complexity comparison of different Viterbi detectors used in each scheme.*

Scheme	Number of states	Number of branch metrics
1D target	4	1
Zero-corner 2D target	4	3
Symmetric 2D target	36	6
Asymmetric 2D target	64	8

complexity.

5. CONCLUSION

At high recording densities, bit-patterned media recording systems experience severe ITI, media noise, and TMR. We proposed the design of the 2D cross-track asymmetric target and its corresponding 1D equalizer, based on an MMSE approach, to combat these disturbances. Based on simulations, at low areal densities (≤ 2 Tbit/in^2) when ITI is small, the 1D target can perform sufficiently well if compared to the 2D target. However, at high areal densities (> 2 Tbit/in^2) when ITI is severe, the 2D target must be employed instead of the 1D target. Furthermore, we found that media noise and TMR cause the 2D BPM pulse response to be asymmetric. Thus, in this situation, the BPMR system must utilize the proposed 2D target to obtain the best performance.

However, it should be noted that the proposed 2D target requires the 2D full-complexity Viterbi detector. Consequently, there is a trade-off between performance improvement and increased complexity, when using the proposed 2D target in the BPMR system. Consequently, all advantages gained by the proposed 2D target need to be balanced against the increased implementation cost caused by the 2D full-complexity Viterbi detector.

ACKNOWLEDGMENT

This project was financially supported by National Research Council of Thailand, Thailand.

References

[1] S. Nabavi, "Signal processing for bit-patterned media channel with inter-track interfence," Ph.D. dissertation, Dept. Elect. Eng. Comp. Sci., Carnegie Mellon University, Pittsburgh, PA, 2008.

[2] Y. Shiroishi, K. Fukuda, *et al.*, "Future options for HDD storage," *IEEE Trans. Magn.*, vol. 45, no. 10, pp. 3816–3822, October 2009.

[3] T. Rausch, J. A. Bain, D. D. Stancil, and T. E. Schelesinger, "Thermal Williams-Comstock model for predicting transition length in a heat-assisted magnetic recording system," *IEEE Trans. Magn.*, vol. 40, no. 1, pp. 137–147, January 2004.

[4] J. G. Zhu, X. Zhu, and Y. Tang, "Microwave assisted magnetic recording," *IEEE Trans. Magn.*, vol. 44, no. 1, pp. 125–131, January 2008.

[5] W. Chang and J. R. Cruz, "Inter-track interference mitigation for bit-patterned magnetic recording," *IEEE Trans. Magn.*, vol. 46, no. 11, pp. 3899–3908, November 2010.

[6] R. Wood, M. Williams, A. Kavcic, and J. Miles, "The feasibility of magnetic recording at 10 terabits per square inch on conventional media," *IEEE Trans. Magn.*, vol. 45, no. 2, pp. 917–923, February 2009.

[7] G. D. Forney, "Maximum-likelihood sequence estimation of digital sequences in the presence of intersymbol interference," *IEEE Trans. Inform. Theory*, vol. IT-18, no. 3, pp. 363-378, May 1972.

[8] J. Moon and W. Zeng, "Equalization for maximum likelihood detector," *IEEE Trans. Magn.*, vol. 31, no. 2, pp. 1083–1088, March 1995.

[9] S. Nabavi, B. V. K. Kumar, and J. G. Zhu, "Modifying Viterbi algorithm to mitigate intertrack interference in bit-patterned media," *IEEE Trans. Magn.*, vol. 43, no. 6, pp. 2274–2276, June 2007.

[10] S. Nabavi, B. V. K. Kumar, and J. A. Bain, "Mitigating the effect of track misregistration in bit-patterned media," in *Proc. IEEE Int. Conf. Commun. 2008.*, Beijing, Chinna, pp. 2061–2065.

[11] S. Karakulak, "From channel modeling to signal processing for bit-patterned media recording," Ph.D dissertation, Deparment of Electrical Engineering, University of Clofornia, San Diego, 2010.

[12] L. M. M. Myint, P. Supnithi, and P. Tantaswadi, "An inter-track interference mitigation technique using partial ITI estimation in patterned media storage," *IEEE Trans. Magn.*, vol. 45, no. 10, pp. 3691–3694, October 2009.

[13] S. Koonkarnkhai, N. Chirdchoo, and P. Kovintavewat , "Iterative decoding for high-density bit-patterned media recording," *Procedia Engineering* (32), pp. 323–328, March 2012.

[14] M. Keskinoz, "Two-dimensional equalization/detection for patterned media storage," *IEEE Trans. Magn.*, vol. 44, no. 4, pp. 533–539, April 2008.

Santi Koonkarnkhai received the B.Eng. degree in Electronics Engineering Technology (2006) and the M.Eng. degree in Electrical Engineering (2009), all from King Mongkut's University of Technology North Bangkok, Thailand. He is currently a doctoral student at King Mongkut's University of Technology North Bangkok. His research interests include communication systems and signal processing for data storage systems.

Phongsak Keeratiwintakorn received his Master's degree from University of Kansas, Lawrence, KS, USA. in 2000 and Ph.D. from University of Pittsburgh, Pittsburgh, PA, USA, in 2005. During his study, he was also a research assistant from 1997-2000 at University of Kansas and from 2000 - 2005 at University of Pittsburgh. Currently, he is an assistant professor at King Mongkut's University of Technology North Bangkok, Bangkok, Thailand. His current research area is Digital Signal Processing, Wireless Communication Systems, Wireless Network Security, Wireless Sensor Networks, and Short Range Communication. He has been an IEEE member since 1997.

Piya Kovintavewat received the B.Eng. summa cum laude from Thammasat University, Thailand (1994), the M.S. degree from Chalmers University of Technology, Sweden (1998), and the Ph.D. degree from Georgia Institute of Technology, USA (2004), all in Electrical Engineering. He is currently Nakhon Pathom Rajabhat University. His research interests include coding and signal processing as applied to digital data storage systems. Prior to working at NPRU, he worked as an engineer at Thai Telephone and Telecommunication company (1994-1997), and as a research assistant at National Electronics and Computer Technology Center (1999), both in Thailand. He also had work experiences with Seagate Technology, Pennsylvania, USA (summers 2001, 2002, and 2004).